

Effect of Immersion Time on the Copper Corrosion in Neutral NaCl Solution

H.X. Liu, B.Y. Hu, Y. Chen*, Y.W. Liu, Y. Xie, L. Zhang, Z.N. Yang*

Department of Chemical Engineering and Safety, Binzhou University, Binzhou, Shandong 256600, China

*E-mail: chen123yu123@163.com (Y. Chen); yangzhongnian@126.com (Z.N. Yang)

Received: 31 March 2018 / *Accepted:* 27 April 2018 / *Published:* 5 June 2018

This paper deals with the investigation of the effect of immersion time on copper corrosion in neutral NaCl solution in presence of benzotriazole using electrochemical impedance spectroscopy (EIS) and electrochemical noise analysis (ENA). EIS results indicated that the corrosion process of copper in neutral NaCl solution in presence of benzotriazole can be classified into five steps in our experimental condition. New parameter of corrosion active energy C_{AE} is proposed from EN analysis to further study the effect of immersion time on copper corrosion in neutral NaCl solution in presence of benzotriazole, which almost shows the opposite variation trend with charge transfer resistance with immersion time.

Keywords: inhibition; benzotriazole; electrochemical noise; long-term effect

1. INTRODUCTION

Due to its excellent mechanical and electric properties, copper has been one of the most popular materials in industry. Although copper is relatively noble compared with other metals, it is susceptible to corrosive species such as chloride, sulfate and nitrate ions. Benzotriazole (BTAH) has been paid much attention for decades as one of the most effective corrosion inhibitors for copper and its alloys [1-18]. It is generally believed that BTAH can form a protective film by two different types of mechanisms. The first postulated chemical adsorption of BTAH on copper surface which acted as the protective barrier to retard the corrosion [19-22] and the second predicted the formation of copper-benzotriazole polymeric film on the surface of the electrode [23-26]. It was also proposed that these two inhibition mechanisms were connected. The adsorption of BTAH is favored at a low inhibitor concentration, low pH and negative electrode potential, whereas the formation of insoluble polymeric film occurs at a high inhibitor concentration, higher pH and positive electrode potential [27].

The inhibition behavior of BTAH on copper has been investigated in different environments, such as acidic solutions [28-30], neutral and alkaline solutions [31-33], synthetic sea water [34] and so

on. In slightly acidic environments, benzotriazole is present mainly in the undissociated form as BTAH, whilst at alkaline pH the molecule is predominantly present in the BTA^- form [2]. Furthermore, the film growth could be best represented by a logarithmic law at high pH values, which changed to a parabolic law at neutral and mildly acidic pH and finally to a dissolution-precipitation mechanism at pH 2 [23].

The aim of this work is to examine the inhibition behavior of BTAH on copper in NaCl aqueous solution using EIS and EN measurements, especially investigate the effect of immersion time. In addition, a new parameter from EN analysis was proposed to evaluate the inhibition efficiency and corrosion severity, which almost exhibited the opposite variation trend with charge transfer resistance during the whole immersion time. There is not a lot of data in the literature related to the effect of immersion time on the corrosion behavior of copper in NaCl aqueous solution containing BTAH inhibitor. Thus, this work will enable a deeper insight into this phenomenon.

2. EXPERIMENTAL

The electrolyte of 0.1 M NaCl solution was prepared from analytical grade chemical NaCl and double distilled water. 40 mg/L benzotriazole (Aladdin, 99%) was added into this solution to obtain inhibitive samples. Prior to each test, the solution was bubbled with N_2 for 1 h. A cylindrical copper rod (purity = 99.99%) embedded in Teflon holder with an exposed area of 0.50 cm^2 was employed in electrochemical tests as the working electrode. Before each experiment, the copper specimen was polished with different grits of emery paper and alumina powder, rinsed with double distilled water, degreased with acetone, dried in N_2 and finally stored in desiccator for use.

Electrochemical experiments were carried out in a conditional three-compartment cell. A large platinum foil and saturated calomel electrode (SCE) connected through a salt bridge was employed as counter and reference electrode, respectively. Electrochemical impedance spectroscopy (EIS) was performed over the frequency range from 100,000 Hz down to 0.01 Hz using an impedance measurement unit (PARSTAT 2273, Advanced Electrochemical System). The sine voltage perturbation was 5 mV in amplitude.

Electrochemical potential noise generated during copper corrosion in 0.1 M NaCl solution in presence of 40 mg/L BTAH at different immersion time was recorded with a commercial PowerLab coupled with GP Amp (ADInstruments Pty Ltd., Australia) at a sampling rate of 4 Hz. All the measurements were performed in a quiescent solution and the experimental device was shielded in a Faradaic cage. Each case was performed at least three times and the average values were reported.

3. RESULTS AND DISCUSSION

3.1 EIS measurements

EIS diagrams (**Fig.1- Fig.5**) were recorded at the open-circuit potential for copper in 0.1 M NaCl solution in presence of 40 mg/L BTAH at different immersion time. It is obvious that the EIS diagrams exhibit different features during different immersion times. The time-constant numbers of

EIS diagrams have been determined through both the features of the EIS diagrams (such as the number of the phase angle peak in Bode plot, the number of the slopes in Bode plot and the number of the capacitance in Nyquist plot), and the method developed by Wit [35,36] simultaneously. It can be seen that EIS diagrams contain two time constants during initial 240 h, which can be expressed mainly as a charge transfer process and a protective film formed on copper surface [37]. After 240 h, a Warburg diffusion element appears, indicating that the corrosion process is diffusion controlled. Accordingly, the corresponding equivalent electrical circuit (EEC) of the system as depicted in **Fig.6** is used to quantitatively analyze the EIS data with Z-view software, and the fitted results are listed in **Table 1-5**.

It is noticeable that the centers of depressed semi-circle are below the real axis for all Nyquist plots which is known as “frequency dispersion” and related to the roughness and inhomogeneity of the electrode surface, suggesting the replacement of capacity by a constant phase element [38]. The impedance of the constant phase element can be expressed by the following equation [39-41]:

$$Z_{CPE} = \frac{1}{Y_0(j\omega)^n} \quad (1)$$

where Y_0 is the magnitude of the CPE, j is an imaginary number, ω is the angular frequency, and n is the phase shift which represents a degree of surface inhomogeneity whose value lies between 0 and 1. The general unit for CPE is in $\Omega^{-1} s^n cm^{-2}$.

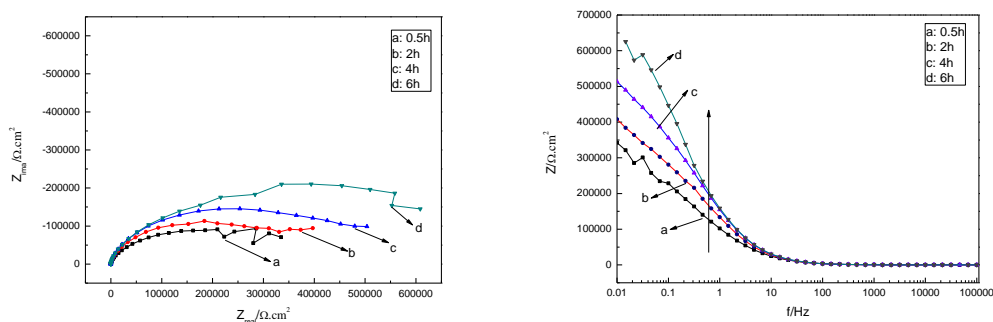


Figure 1. EIS plots of copper in 0.1 M NaCl solution in presence of 40 mg/L BTAH at the initial 6 h immersion time.

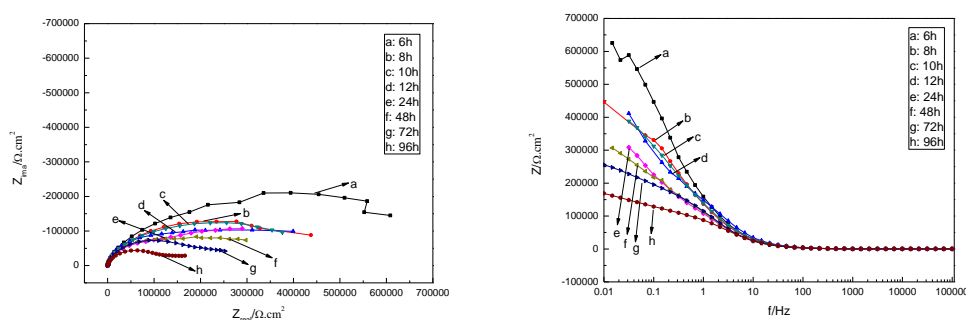


Figure 2. EIS plots of copper in 0.1 M NaCl solution in presence of 40 mg/L BTAH at the immersion time from 6 h to 96 h.

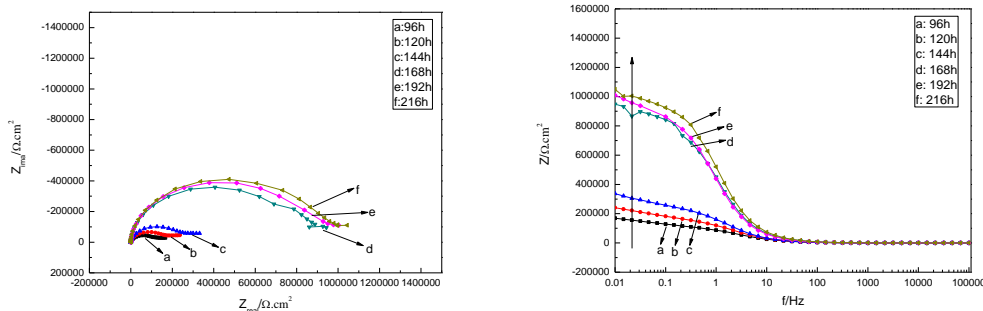


Figure 3. EIS plots of copper in 0.1 M NaCl solution in presence of 40 mg/L BTAH at the immersion time from 96 h to 216 h.

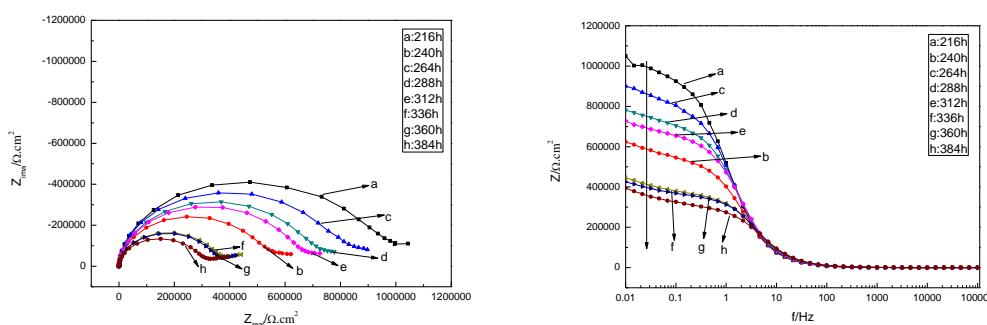


Figure 4. EIS plots of copper in 0.1 M NaCl solution in presence of 40 mg/L BTAH at the immersion time from 216 h to 384 h.

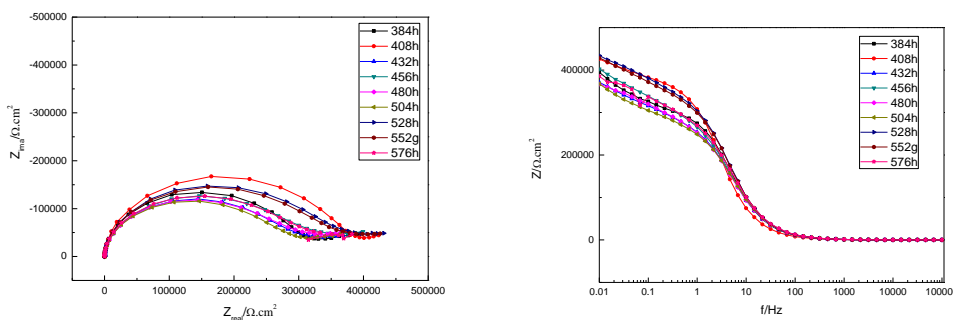
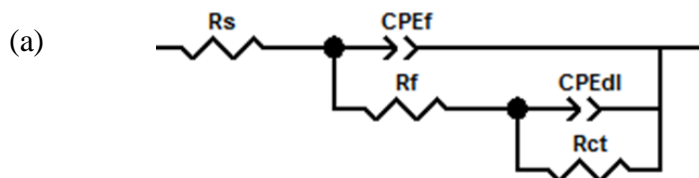


Figure 5. EIS plots of copper in 0.1 M NaCl solution in presence of 40 mg/L BTAH at the immersion time from 384 h to 576 h.



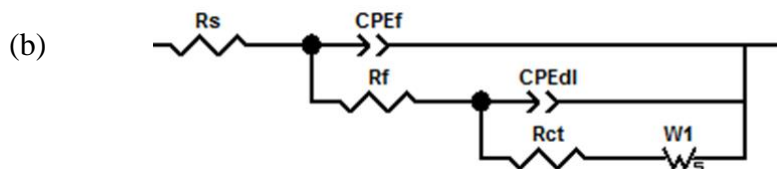


Figure 6. EEC used for simulating the impedance spectra. (a) the initial 240 h; (b) after 240 h immersion time. R_s is the solution resistance, CPE_f is the film capacitance, R_f is the surface film resistance, CPE_{dl} represents the double layer capacitance, R_{ct} is the charge transfer resistance and W_1 is the Warburg diffusion element.

Table 1. EIS analyzed results for copper in 0.1 M NaCl solution with 40 mg/L BTAH at initial 6 h.

Time/h	R_f $k\Omega.cm^2$	CPE_f $\Omega^{-1} s^n cm^{-2}$	n_f	R_{ct} $k\Omega.cm^2$	CPE_{dl} $\Omega^{-1} s^n cm^{-2}$	n_{dl}
0.5	1.40	0.47	0.98	403	2.82	0.85
2	1.86	0.46	0.98	463	1.83	0.86
4	3.72	0.45	0.98	654	1.59	0.81
6	8.21	0.52	0.96	749	1.63	0.83

Table 2. EIS analyzed results for copper in 0.1 M NaCl solution in presence of 40 mg/L BTAH at immersion time from 8 h to 96 h.

Time/h	R_f $k\Omega.cm^2$	CPE_f $\Omega^{-1} s^n cm^{-2}$	n_f	R_{ct} $k\Omega.cm^2$	CPE_{dl} $\Omega^{-1} s^n cm^{-2}$	n_{dl}
8	27.5	0.48	0.98	562	1.73	0.85
10	36.8	0.47	0.97	495	3.96	0.89
12	51.5	0.49	0.97	463	2.21	0.84
24	50.3	0.63	0.96	464	4.46	0.81
48	50.3	0.63	0.97	427	4.46	0.81
72	44.2	0.62	0.96	339	3.06	0.80
96	56.9	0.59	0.97	306	2.15	0.84

It is can be seen from **Table 1-5** that the effect of immersion time on copper corrosion in presence of benzotriazole can be classified into five steps in our experimental condition: (1) the immersion time of 6 h corresponds to the initial film formation process of BTAH on copper surface mainly with chemisorptions mechanism. With prolonging immersion time, more and more BTAH molecules adsorbed onto copper surface to form a protective barrier which resulted into the increase of the charge transfer resistance R_{ct} ; (2) the charge transfer resistance R_{ct} decreases with prolonging the immersion time from 6 h to 96 h, which may be ascribed to the desorption of BTAH molecules on copper surface and the dissolution of copper as well; (3) during the immersion time from 120 h to 216

h, the charge transfer resistance R_{ct} increases with immersion time, suggesting the formation of copper-benzotriazole polymeric film [Cu(I)BTA] on the copper surface to retard the corrosive attack; (4) the charge transfer resistance R_{ct} decreases with the increase of immersion time from 240 h to 384 h; (5) during the immersion time from 408 h to 576 h, the copper surface reaches a relative stable state and the charge transfer resistance fluctuated around a mean value.

Table 3. EIS analyzed results for copper in 0.1 M NaCl solution in presence of 40 mg/L BTAH at immersion time from 120 h to 216 h.

Time/h	R_f k Ω .cm ²	CPE_f $\Omega^{-1} s^n cm^{-2}$	n_f	R_{ct} k Ω .cm ²	CPE_{dl} $\Omega^{-1} s^n cm^{-2}$	n_{dl}
120	45.3	0.49	0.96	366	2.75	0.85
144	69.1	0.49	0.97	502	2.00	0.81
168	105	0.26	0.98	1321	0.48	0.86
192	124	0.28	0.98	1769	0.59	0.82
216	158	0.21	0.98	1925	0.45	0.81

Table 4. EIS analyzed results for copper in 0.1 M NaCl solution in presence of 40 mg/L BTAH at immersion time from 240 h to 384 h.

Time/h	R_f k Ω .cm ²	CPE_f $\Omega^{-1} s^n cm^{-2}$	n_f	R_{ct} k Ω .cm ²	CPE_{dl} $\Omega^{-1} s^n cm^{-2}$	n_{dl}	W k Ω .cm ²
240	163	0.21	0.98	594	2.41	0.84	189
264	209	0.21	0.98	1081	1.61	0.85	292
288	179	0.19	0.98	856	1.81	0.81	254
312	260	0.19	0.98	639	2.27	0.81	226
336	189	0.18	0.98	375	2.90	0.83	195
360	172	0.17	0.98	349	0.59	0.81	131
384	210	0.16	0.98	260	3.46	0.83	97.2

Table 5. EIS analyzed results for copper in 0.1 M NaCl solution in presence of 40 mg/L BTAH at immersion time 408 h to 576 h.

Time/h	R_f k Ω .cm ²	CPE_f $\Omega^{-1} s^n cm^{-2}$	n_f	R_{ct} k Ω .cm ²	CPE_{dl} $\Omega^{-1} s^n cm^{-2}$	n_{dl}	W k Ω .cm ²
408	196	0.15	0.98	369	2.07	0.84	193
432	181	0.15	0.98	292	1.79	0.81	217
456	180	0.15	0.98	297	1.60	0.83	299
480	119	0.15	0.98	260	1.66	0.85	265
504	124	0.14	0.98	351	1.20	0.82	241
528	152	0.14	0.98	302	1.44	0.84	237
552	113	0.14	0.98	367	1.37	0.81	235
576	138	0.14	0.98	260	1.71	0.83	224

3.2 EN analysis

Fig.7- Fig.11 shows the electrochemical potential noise of copper corroded in 0.1 M NaCl solution in presence of 40 mg/L BTAH at different immersion time. In the case of electrochemical potential noise, the mean value is the corrosion potential [42]. It can be seen that the corrosion potential almost moves in the positive direction during the whole immersion time. In addition, the EN curves show different features with different immersion time. It is apparent that EN generated in the initial 96 h (**Fig.7** and **Fig.8**) had large noise amplitude, while possessed small potential oscillation amplitude after immersion for 96 h. There exists a competition between the adsorption of BTAH onto copper surface and the dissolution of copper, which causes the oscillation / fluctuation of the corrosion potential. In the initial 96 h, the adsorption of BTAH and dissolution of copper occurred simultaneously on the copper surface. With increasing immersion time, a more compact and stable protective film formed on the copper surface and resisted the permeation of corrosive Cl^- through this film to reach the copper surface.

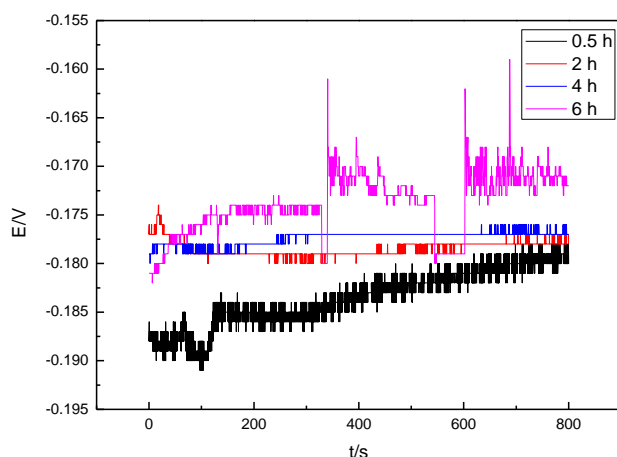


Figure 7. Electrochemical potential noise of copper in 0.1 M NaCl solution in presence of 40 mg/L BTAH at the initial 6 h immersion time.

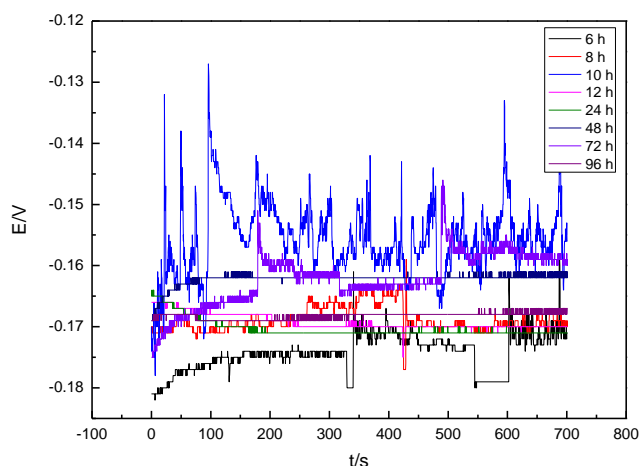


Figure 8. Electrochemical potential noise of copper in 0.1 M NaCl solution in presence of 40 mg/L BTAH at the immersion time from 6 h to 96 h.

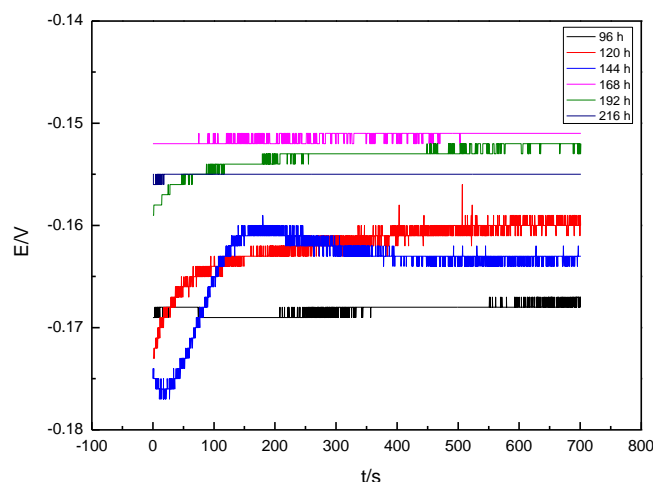


Figure 9. Electrochemical potential noise of copper in 0.1 M NaCl solution in presence of 40 mg/L BTAH at the immersion time from 96 h to 216 h.

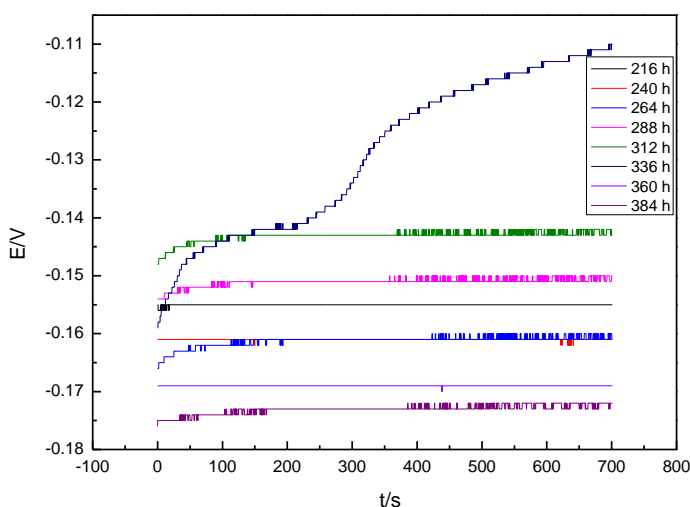


Figure 10. Electrochemical potential noise of copper in 0.1 M NaCl solution in presence of 40 mg/L BTAH at the immersion time from 216 h to 384 h.

In order to quantitatively detect the EN features and inhibition behavior of BTAH on copper, wavelet transformation of the orthogonal Daubechies wavelets (FWT) of the fourth order (db4) was used to analyze the noise data containing 5120 points. The theoretical algorithm was expressed in detail in literature [22,43] as shown in **Fig.12**.

Based on the FWT theoretical algorithm, a time record $x_i(t) (i = 1, 2, \dots, N)$ can be expressed using a linear combinations of basis functions $\Phi_{j,k}$ and $\varphi_{j,k}$ and amplitude coefficients of each function $S_{j,k}, D_{j,k}, \dots, D_{l,k}$

$$x(t) \approx \sum_k S_{j,k} \Phi_{j,k}(t) + \sum_k D_{j,k} \varphi_{j,k}(t) + \sum_k D_{j-1,k} \varphi_{j-1,k}(t) + \dots + \sum_k D_{1,k} \varphi_{1,k}(t) \quad (2)$$

$$S_{j,k} = \int x(t) \Phi_{j,k}^*(t) dt \quad (3)$$

$$D_{l,k} = \int x(t) \varphi_{l,k}^*(t) dt \quad (4)$$

Where $\varphi_{j,k}^*$ and $\varphi_{l,k}^*$ are the complex conjugate of the basis functions father wavelet $\varphi(t)$ and mother wavelet $\varphi(t)$, which is the basis for this decomposition through translating and scaling as follows:

$$\varphi_{j,k}(t) = 2^{-j/2} \varphi(2^{-j}t - k) = 2^{-j/2} \varphi\left(\frac{t-2^j k}{2^j}\right) \quad (5)$$

$$\varphi_{j,k}(t) = 2^{-l/2} \varphi(2^{-l}t - k) = 2^{-l/2} \varphi\left(\frac{t-2^l k}{2^l}\right) \quad (6)$$

Where $k = 1, 2, \dots, N/2$, N corresponds to the number of data record. $l = 1, 2, \dots, J$, J is often a small natural number. Moreover, 2^l is related to the scale factor and $2^l k$ corresponds to translation parameter.

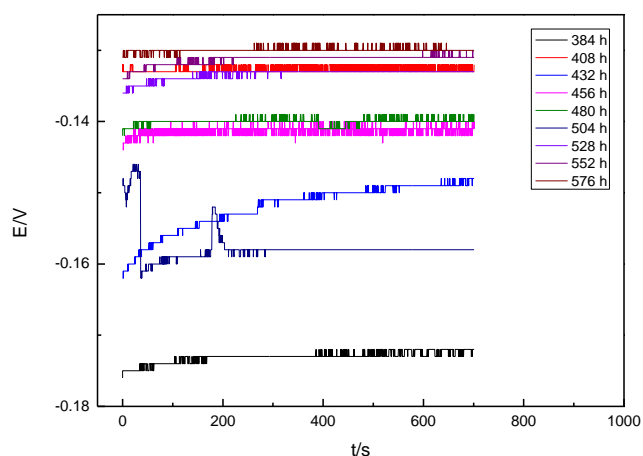


Figure 11. Electrochemical potential noise of copper in 0.1 M NaCl solution in presence of 40 mg/L BTAH at the immersion time from 384 h to 576 h.

It can be seen from **Fig.12** that the discrete signal $x_i(t) (i = 1, 2, \dots, N)$ is initially decomposed into two sets of coefficients by low-pass filter (L) and high-pass filter (H): the first smooth coefficient set $S_i = (S_1, S_2, \dots, S_j)$ contains the information about the general trend of the original signal and the second detail coefficient set $D_i = (D_1, D_2, \dots, D_j)$ encodes the information about the local features of the original signal. After filtering, the outputs are then down-sampled ($2 \downarrow$), meaning deleting one of every two consecutive sample of the filtered components. Finally, the smooth coefficients S_i and detail coefficients D_i are saved, each of which is called a crystal and related to the features of the original signal [44-46].

Therefore, the overall energy (E) of the noise containing 5120 data points in our experiment was calculated as follows:

$$E = \sum_{n=1}^N S_n^2 (n = 1, 2, \dots, N, N = 5120) \quad (7)$$

Then, the fraction of energy associated with each crystal (D and S) can be calculated by the following equation:

$$E_l^D = \frac{1}{E} \sum_{k=1}^{N/2^l} D_{l,k}^2 \quad (l = 1, 2, \dots, J, J = 8) \quad (8)$$

$$E_J^S = \frac{1}{E} \sum_{k=1}^{N/2^J} S_{J,k}^2 \quad (l = 1, 2, \dots, J) \quad (9)$$

Since the chosen wavelets are orthogonal, the following equation is satisfied:

$$E = E_J^S + \sum_{l=1}^J E_l^D \quad (10)$$

The plots of each crystal and its corresponding relative energy are depicted as the energy distribution plots (EDPs). Furthermore, in order to remove the energy contribution of dc drift from the ensemble energy of the noise, the EDP was re-plotted by discounting the energy contribution of S₈ crystal from the ensemble signal energy, i.e., removing the large voltage transient from the raw EN data [47]. The thus obtained re-plotted EDPs (RP-EDPs) are shown in **Fig.13-17**.

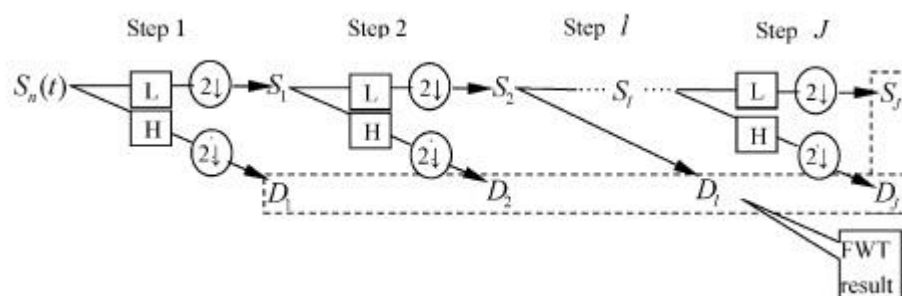


Figure 12. Theoretical algorithm scheme of the fast wavelet transform.

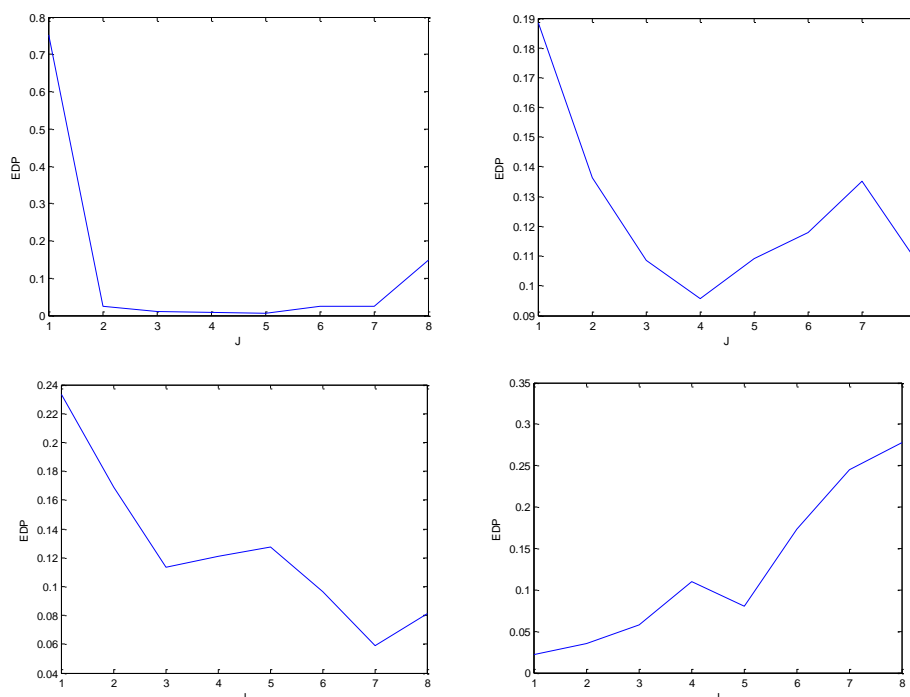


Figure 13. RP-EDP generated during copper corrosion in 0.1 M NaCl solution in the presence of 40 mg/L BTAH at the initial 6 h immersion time.

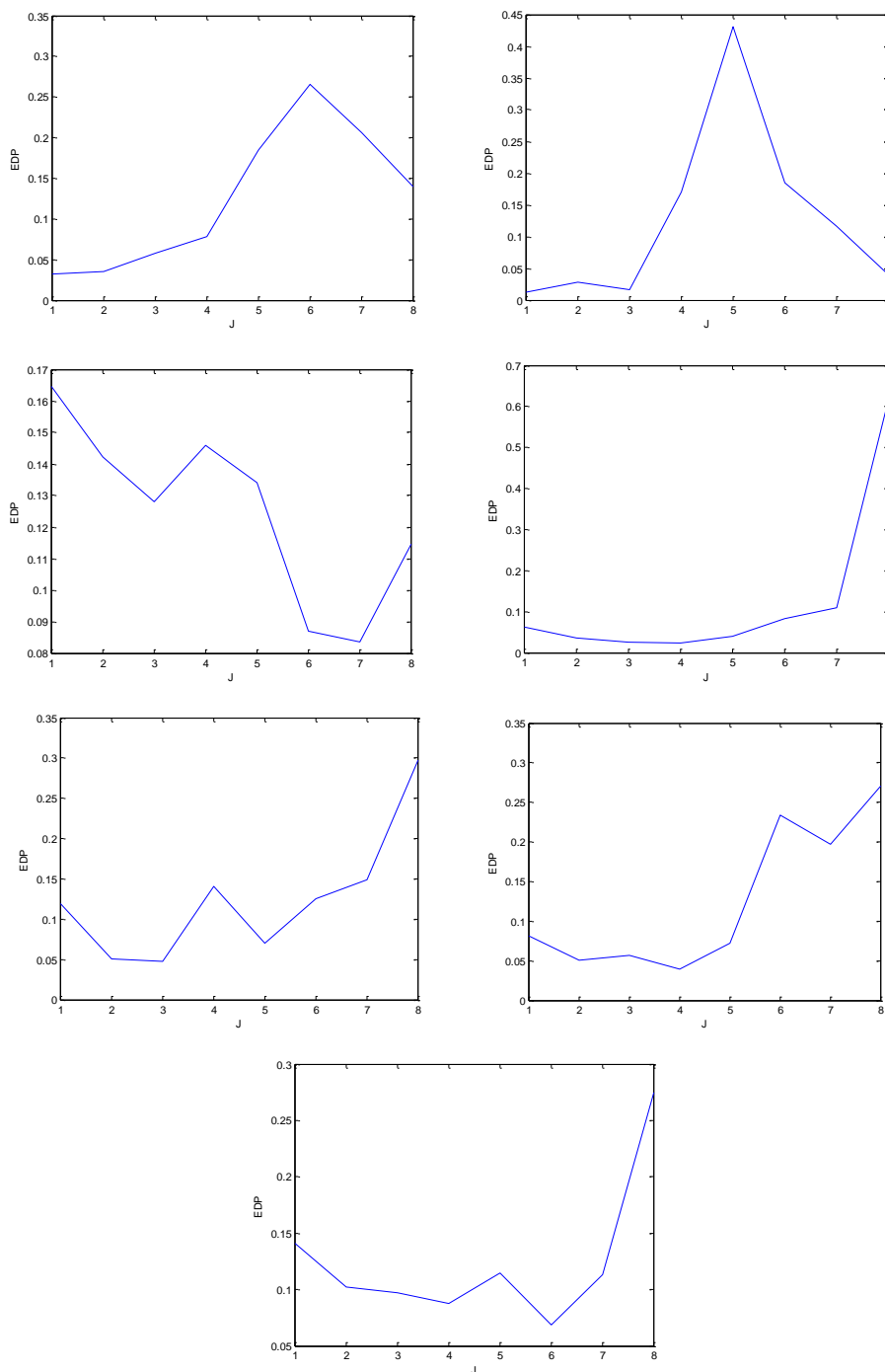


Figure 14. RP-EDP generated during copper corrosion in 0.1 M NaCl solution in the presence of 40 mg/L BTAH at the immersion time from 8 h to 96 h.

The wavelet coefficient represents the time-scale characteristics of the associated corrosion event [48]. Generally, smaller timescales correspond to a reasonably fast phenomenon at higher frequency range (e.g. metastable pitting) and a relatively slow process is related to larger timescales in the lower frequency domain (e.g. general corrosion) [49]. Moreover, the metastable pitting process occurs always before its propagation[50], it is rational to divide the RP-EDP plot into three segments

[49,50]: 1) region A between D_1 and D_3 in the higher frequency domain mainly characterizes a reasonably fast phenomenon (e.g. pitting nucleation), 2) region B between D_3 and D_6 mainly characterizes the pitting development, and 3) region C between D_6 and D_8 at lower frequency range corresponds to a relatively slow process (e.g. diffusion process).

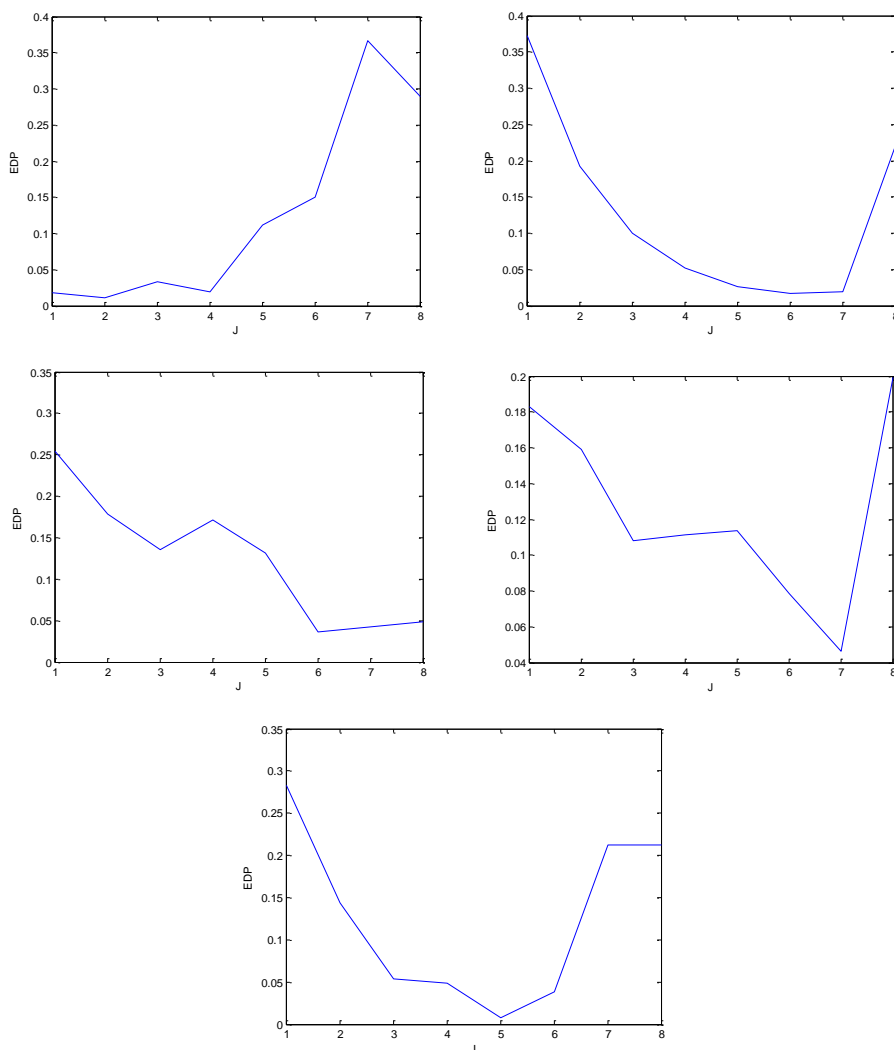
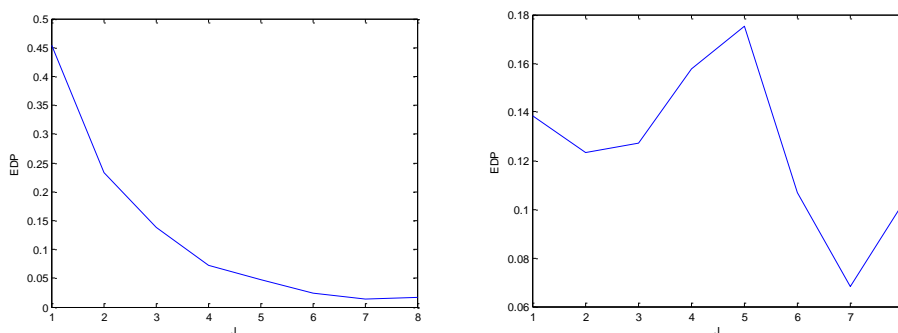


Figure 15. RP-EDP generated during copper corrosion in 0.1 M NaCl solution in the presence of 40 mg/L BTAH at the immersion time from 120 h to 216 h.



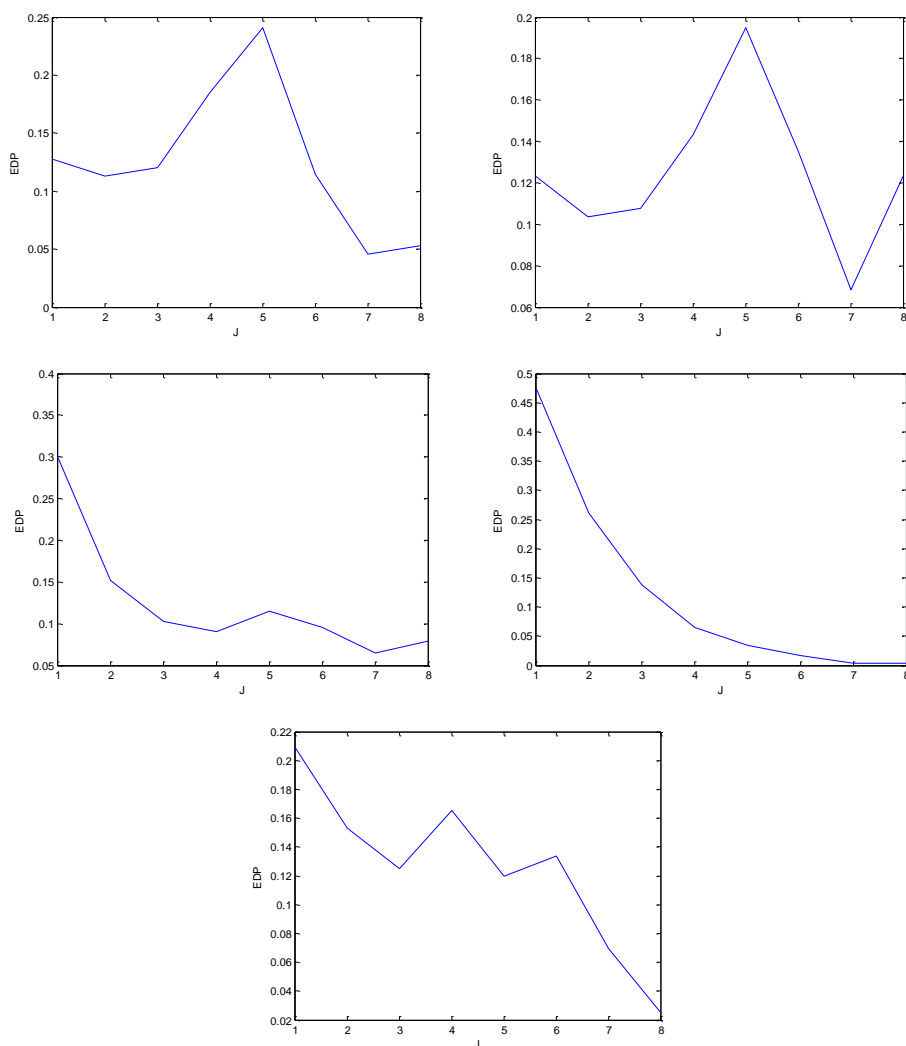
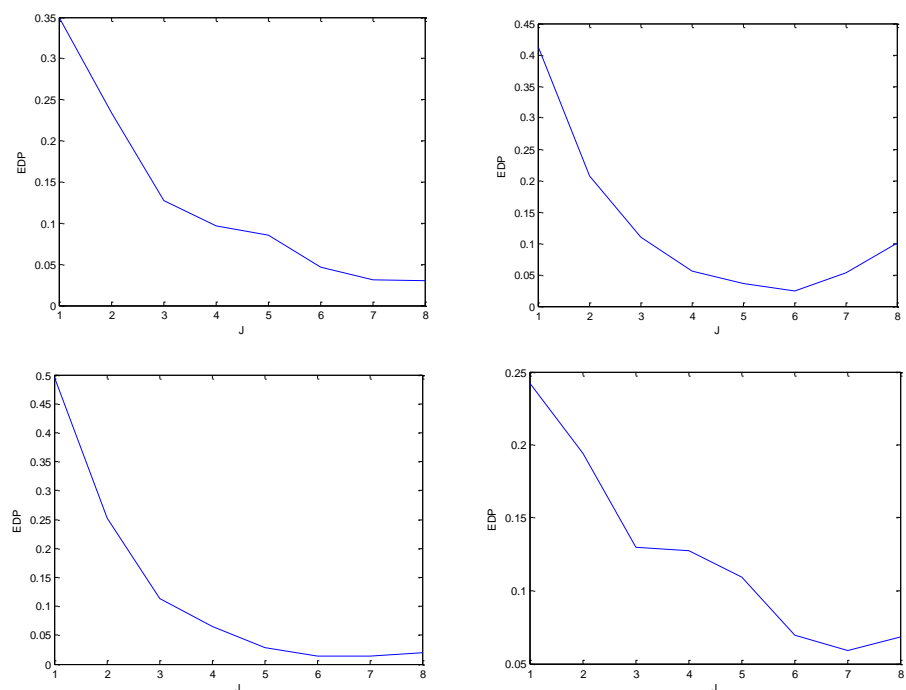


Figure 16. RP-EDP generated during copper corrosion in 0.1 M NaCl solution in the presence of 40 mg/L BTAH at the immersion time from 240 h to 384 h.



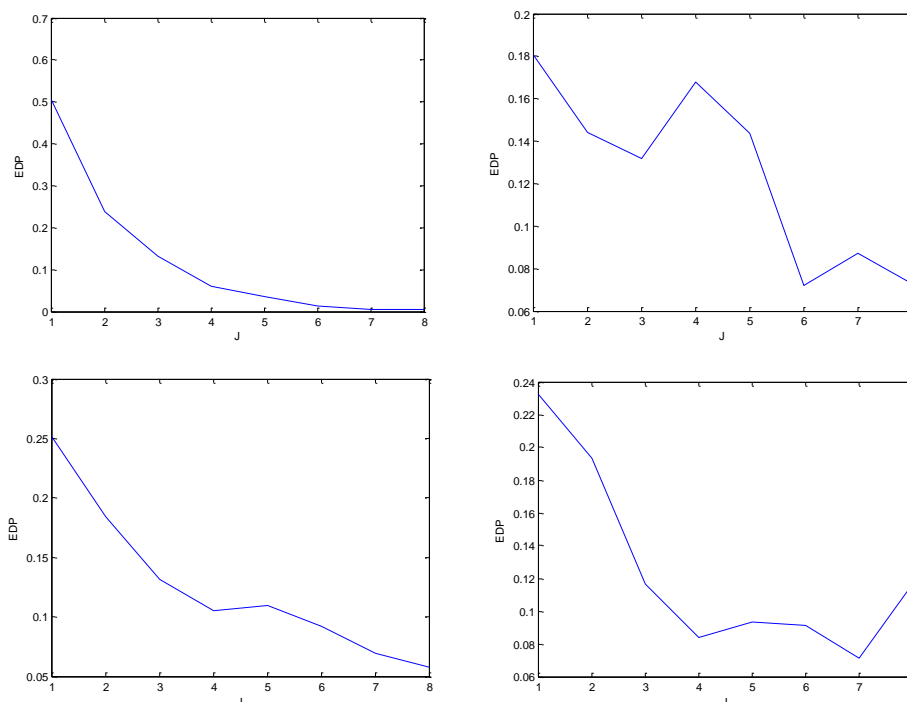


Figure 17. RP-EDP generated during copper corrosion in 0.1 M NaCl solution in the presence of 40 mg/L BTAH at the immersion time from 408 h to 576 h.

It is interesting from **Fig.13-17** that the energy is mainly deposited in the higher frequency domain (region A and B) after immersion time of 240 h, indicating that the copper corrosion process is diffusion controlled [48], which result matches well with that of the EIS measurements. However, it is unfortunate that the characteristic of the RP-EDP plots generated during the whole immersion time (**Fig.13-17**) is still obscure to provide more useful information about the effect of immersion time on copper corrosion in presence of benzotriazole in 0.1 M NaCl solution.

Therefore, it is necessary to set up a new parameter or method to detect such inappreciable changes in RP-EDP plots during the whole immersion time, which should have a direct utility for monitoring the inhibitor behavior of BTAH on copper surface. A new parameter C_{AE} named the corrosion active energy which represents the electrochemical reaction rate, is defined as follows to evaluate the inhibition behavior [22],

$$C_{AE} = E_{d1} + E_{d2} + E_{d3} + E_{d4} + E_{d5} + E_{d6} \tag{11}$$

where $E_{d1} + E_{d2} + E_{d3}$ is the energy related to the pitting nucleation process in region A, $E_{d4} + E_{d5} + E_{d6}$ is the energy corresponding to the pitting growth process in region B.

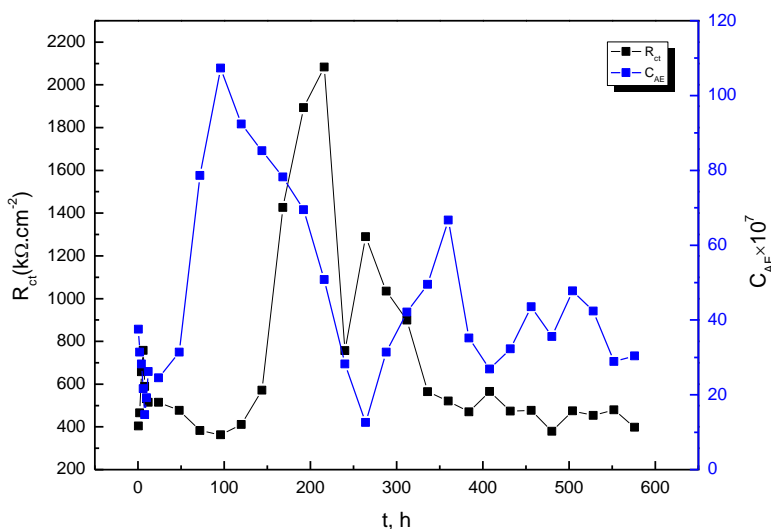
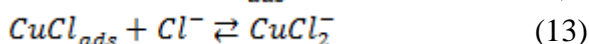
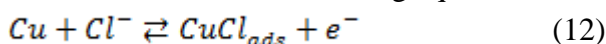


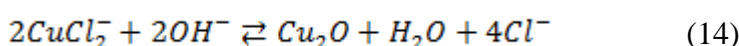
Figure 18. Dependence of R_{ct} and corrosion active energy C_{AE} on immersion time.

The dependence of the charge transfer resistance R_{ct} and corrosion active energy C_{AE} on immersion time is shown in **Fig.18**. Interestingly, it can be seen that the value of this new defined parameter C_{AE} almost shows the opposite variation trend of R_{ct} with immersion time.

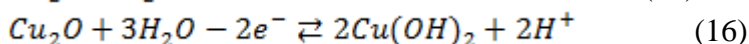
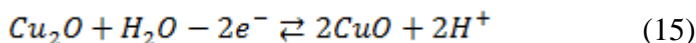
The dissolution of copper in near neutral chloride solution has been presented in the polarization section with the following equations:



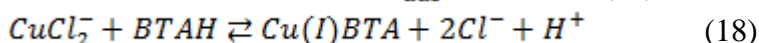
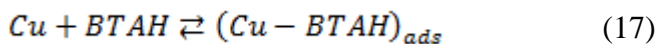
Then, Cu_2O is formed by the hydrolysis process of $CuCl_2^-$ [51]:



Subsequently, Cu_2O will further convert to CuO and/or $Cu(OH)_2$ by the following mechanism [52]:



When BTAH is added into the treated solution, the inhibition mechanism of BTAH onto copper surface can be expressed as follows [53]:



In the initial 6 h immersion time, equation (17) is dominant that a protective film of $(Cu - BTAH)_{ads}$ formed on the copper surface in presence of 40 mg/L BTAH in 0.1 M NaCl solution although the competitive reaction of equation (12) coexists, resulting into the increase of charge transfer resistance R_{ct} and decrease of corrosion active energy C_{AE} . With increasing immersion time from 6 h to 96 h, the potential difference between Cu and $(Cu - BTAH)_{ads}$ will certainly accelerate the corrosion process of copper. In other words, the active sites on the copper surface without BTAH molecules will be attacked by the corrosive Cl^- ions with equation (12). The competition between the

forming of $(\text{Cu-BTAH})_{\text{ads}}$ film on copper surface and the dissolution of copper will certainly cause the large oscillation / fluctuation of the corrosion potential (**Fig.8**). Lately, the corrosion products of CuCl_2^- will further convert to insoluble Cu(I)BTA film in the presence of 40 mg/L BTAH in 0.1 M NaCl solution which reaction rate is much larger than the dissolution rate of equation (14), contributed to the increase of charge transfer resistance. After that, the formation of Cu(I)BTA film and dissolution process reached equilibrium, and the copper surface came to a relatively steady state. Thus, the charge transfer resistance and the corrosion active energy C_{AE} fluctuated around a mean value.

4. CONCLUSIONS

The effect of immersion time on copper corrosion in neutral NaCl solution in presence of benzotriazole has been studied by electrochemical impedance spectroscopy (EIS) and electrochemical noise analysis (ENA). The inhibition behavior can be classified into five steps from the EIS results. New parameter C_{AE} proposed from EN analysis, corresponding to the corrosion active energy, was presented to further study the effect of immersion time on copper corrosion in neutral NaCl solution in presence of benzotriazole. The corrosion active energy C_{AE} almost showed the opposite variation trend with charge transfer resistance with immersion time.

ACKNOWLEDGEMENTS

The authors wish to acknowledge the financial supports of the National Natural Science Foundation of China (Project 21403194), the Doctoral Research Foundation of Binzhou University (2017Y01), Scientific Research Fund of Binzhou University (BZXYZZJJ201604), National Training Programs of Innovation and Entrepreneurship (201710449016, 201710449017), and the Major Project of Binzhou University (2017ZDL02, 2016ZDW03).

References

1. P.G. Fox, G. Lewis, P.J. Boden, *Corros. Sci.* 19 (1979) 457.
2. Matjaž Finšgar, Ingrid Milošev, *Corros. Sci.* 52 (2010) 2737.
3. S. Liu, J.M. Duan, R.Y. Jiang, Z.P. Feng, R. Xiao, *Corrosion*, 62 (2011) 47.
4. D. Gelman, D. Starosvetsky, Y. Ein-Eli, *Corros. Sci.* 82 (2014) 271.
5. G.W. Poling, *Corros. Sci.* 10 (1970) 359.
6. A.M. Abdullah, F.M. Al-Kharafi, B.G. Ateya, *Scr. Mater.* 54 (2006) 1673.
7. I. Dugdale, J.B. Cotton, *Corros. Sci.* 3 (1963) 69.
8. H. Bi, G.T. Burstein, B.B. Rodriguez, G. Kawaley, *Corros. Sci.* 102 (2016) 510.
9. E. Cano. J.L. Polo, A. La Iglesia, J.M. Bastidas, *Adsorption*, 10 (2004) 219.
10. F. Mansfeld, T. Smith, E.P. Parry, *Corrosion*, 27 (1971) 289.
11. L. Tommesani, G. Brunoro, A. Frignani, C. Monticelli, M. Dal Colle, *Corros. Sci.* 39 (1997) 1221.
12. Y.H. Lei, N. Sheng, A. Hyono, M. Ueda, T. Ohtsuka, *Prog. Org. Coat.* 77 (2014) 339.
13. S.M. Milić, M.M. Antonijević, *Corros. Sci.* 51 (2009) 28.
14. G. Xue, J. Ding, *Appl. Surf. Sci.* 40 (1990) 327.
15. D. Tromans, R. Sun, *J. Electrochem. Soc.* 138 (1991) 3235.
16. Gregor Žerjav, Ingrid Milošev, *Corros. Sci.* 98 (2015) 180.

17. N.K. Allam, A.A. Nazeer, E.A. Ashour, *J. Appl. Electrochem.* 39 (2009) 961.
18. K. Cho, J. Kishimoto, T. Hashizume, H. W. Pickering, T. Sakurai, *Appl. Surf. Sci.* 87 (1995) 380.
19. D. Thierry, C. Leygraf, *J. Electrochem. Soc.* 132 (1985) 1009.
20. G. Lewis, *Br. Corros. J.* 16 (1981) 169.
21. Y. Chen, Y.Y. Jiang, Z. Y. Ye, Z. Zhang, *Corrosion*, 69 (2013) 886.
22. Y. Chen, Z.N. Yang, Y.W. Liu, H.H. Zhang, J.Y. Yin, Y. Xie, Z. Zhang, *J. Taiwan. Inst. Chem. E.* 80 (2017) 908-914.
23. Chen. Jin-Hua, Lin. Zhi-Cheng, Chen. Shu, Nie. Li-Hua, Yao. Shou-Zhuo, *Electrochim. Acta*, 43 (1998) 265.
24. A.D. Modestov, G.D. Zhou, Y.P.Wu, T. Notoya, D.P. Schweinsberg, *Corros. Sci.* 36 (1994) 1931.
25. V. Brusic, M.A. Frisch, B.N. Eldridge, F.P. Novak, F.B. Kaufman, B.M. Rush, G.S. Frankel, *J. Electrochem. Soc.* 138 (1991) 2253.
26. M.V. Rylkina, M.V. Didik, *Protect. Metals*, 43 (2) (2007) 179.
27. R. Youda, H. Nishihara, K. Aramaki, *Electrochim. Acta*, 35 (1990) 1011.
28. C. Clerc, R. Alkire, *J. Electrochem. Soc.* 138 (1991) 25.
29. Jeng-Yu Lin, Alan C. West, *Electrochim. Acta*, 55 (2010) 2325.
30. R. Babić, M. Metikoš-Huković, M. Lončar, *Electrochim. Acta*, 44 (1999) 2413.
31. R. Subramanian, V. Lakshminarayanan, *Corros. Sci.* 44 (2002) 535.
32. Nageh K. Allam, Elsayed A. Ashour, *Appl. Surf. Sci.* 254 (2008) 5007.
33. Tadeja Kosec, Ingrid Milošev, Boris Pihlar, *Appl. Surf. Sci.* 253 (2007) 8863.
34. B.V. Appa Rao, K. Chaitanya Kumar, Neha Y. Hebalkar, *Thin Solid Films*, 556 (2014) 337.
35. D.H. van der Weijde, E.P.M. van Westing, J.H.W.de Wit, *Corros. Sci.* 36 (1994) 643.
36. P. Campestrini, E.P.M van Westing, J.H.W de Wit, *Electrochim. Acta*, 46 (2001) 2631.
37. Yan Ji, Bin Xu, Weinan Gong, Xueqiong Zhang, Xiaodong Jin, Wenbo Ning, Yue Meng, Wenzhong Yang, Yizhong Chen, *J. Taiwan. Inst. Chem. E.* 66 (2016) 301.
38. J.R. Macdonald, *J. Electroanal. Chem. Interfacial Electrochem.* 223 (1987) 25.
39. I. Ahamad, R. Prasad, M. Quraishi, *Mater. Chem. Phys.* 124 (2010) 1155.
40. N.D. Nam, Q.V. Bui, M. Mathesh, M.Y.J. Tan, M. Forsyth, *Corros. Sci.* 76 (2013) 257.
41. M. Hazwan Hussin, M. Jain Kassim, N.N. Razali, N.H. Dahon, D. Nasshorudin, *Arab. J. Chem.* 9 (2016) S616.
42. D. Seifzadeh, H. Basharnavaz, A. Bezaatpour, *Mater. Chem. Phys.* 138 (2013) 794.
43. Y.Y. Shi, Z. Zhang, J.X. Su, F.H. Cao, J.Q. Zhang, *Electrochim. Acta*, 51 (2006) 4977.
44. A. Aballe, M. Bethencourt, F.J. Botana, M. Marcos, *Electrochem. Commun.* 1 (1999) 266.
45. Z.H. Dong, X.P. Guo, J.S. Zheng, L.M. Xu, *Electrochem. Commun.* 3 (2001) 561.
46. A. Aballe, M. Bethencourt, F.J. Botana, M. Marcos, *Electrochim. Acta*, 46 (2001) 2353.
47. [X.Q. Huang, Y. Chen, T.W. Fu, Z. Zhang, J.Q. Zhang, *J. Electrochem. Soc.* 160 (2013) D530.
48. [S.M. Hoseinieh, A.M. Homborg, T. Shahrabi, J.M.C. Mol, B. Ramezanzadeh, *Electrochim. Acta*, 217 (2016) 226.
49. C. Cai, Z. Zhang, F.H. Cao, Z.N. Gao, J.Q. Zhang, C.N. Cao, *J. Electroana. Chem.* 578 (2005) 143.
50. M.C. Lefebvre, B.E. Conway, *J. Electroana. Chem.* 480 (2000) 46.
51. G. Kear, B.D. Barker, F.C. Walsh, *Corros. Sci.* 46(2004) 109.
52. D. Tromans, R. Sun, *J. Electrochem. Soc.* 139 (1992) 1945.
53. M. Finšgar, A. Lesar, A. Kokalj, I. Milošev, *Electrochim. Acta*, 53(2008) 8287.